Recent developments in InP and related compounds

Dr Mohamed Henini, University of Nottingham, UK

Although indium phosphide (InP) is hardly known outside the ranks of semiconductor specialists, it must be one of the most thoroughly investigated compound materials known. Over the past few years, great progress has been made in the performance of InP-based devices. Much of this can be attributed to improvement in the quality of the materials from which these devices are fabricated. This article reports on some exciting new results obtained in InP-related materials.

The data on the properties of compounds semiconductors are scattered over many decades in time and many journals. One must spend an inordinate amount of time and effort to gather the information needed. Table 1 shows some useful data on InP.

Recent results

One of the main directions of contemporary semiconductor physics is the production and study of structures with dimension less than two (e.g. quantum wires and dots) in order to realise novel devices that make use of low-dimensional confinement effects.

One of the promising fabrication methods is to use self-organised three-dimensional (3D) structures, such as 3D coherent islands, which are often formed during the initial stage of heteroepitaxial growth in lattice-mismatched systems. Quantum dots (QDs), for example, are believed to provide a promising way for a new generation of optical light sources such as injection lasers. While quantum-well structures are already widely used in optoelectronic devices, quantum wires and quantum boxes appear to be much more difficult to fabricate for this purpose. Work on QD structures is progressing in several laboratories in Japan, the USA, and Europe, and it seems certain that useful QD lasers and other devices will emerge. Clearly, future research work on QDs will connect diverse areas of material science, physics, chemistry and optoelectronics.

H.Li and his co-workers [1] at Duke University, USA, studied self-organised MBE growth of InAs nanowires grown on (100) InP. It was found that dense InAs nanowire arrays could be formed spontaneously. The linear density was as high as 70 wires per micron. The average cross section of the nanowires was 4.5 x 10 nm^2 (see Figures 1 and 2). Wire-like one-dimensional patterns have also been reported in $In_xAl_{1-x}As/In_yAl_{1-y}As$ superlattices on singular (100) InP [2].

Most of the investigations on QDs are focused on structures grown on GaAs substrates. However, the emission wavelength of the InGaAs/GaAs system is limited to the range 0.9-1.3 μm. The InAs/InP system is expected to play an important role in the technologically important optical telecommunication 1.3-1.55 μm wavelength range.

A new class of structures has recently been fabricated which easily reach this range using InP substrates [3]. QDs grown on (311)B InP substrates have been studied by several groups [4-6] in order to fabricate smaller and more uniform QDs sizes, and a higher density than those grown on (100) InP. QD emission wavelength tuning was achieved for 1.55 μm using (311)B InP substrates [6]. S. Hinooda *et al* [7] (INSA de Rennes, France) studied the carrier dynamics of self-assembled InAs QDs grown on (311)B InP substrates. Their QD lateral dimension was about 35 nm and the height about 2 nm. The density was

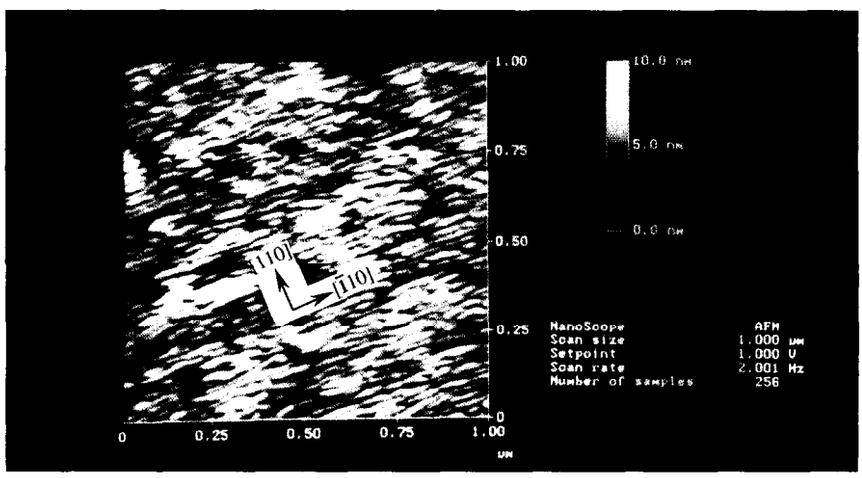

Figure: 1 μm x 1 μm AFM image of the uncapped 6 ML InAs grown on $In_{0.52}Al_{0.48}As$/InP. (Courtesy of H. Li, Duke University, USA)

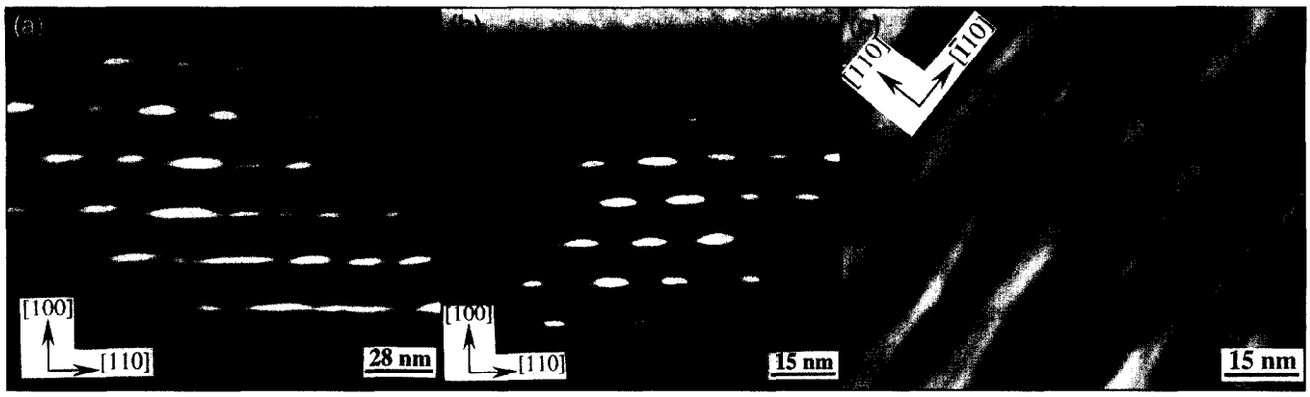

Figure 2: [-110] cross-sectional TEM images of (a) six-period InAs (6.5 ML)/ $In_{0.52}Al_{0.48}As$ (20 nm) nanowire arrays; (b) six-period InAs (6 ML)/ $In_{0.52}Al_{0.48}As$ (10 nm) nanowire arrays; (c) plan-view TEM image of six-period InAs (6 ML)/ $In_{0.52}Al_{0.48}As$ (10 nm) nanowire arrays. (Courtesy of H. Li, Duke University, USA)

estimated to be about $3x10^{10}$ cm^{-2}. By using time-resolved photoluminescence spectroscopy they observed an efficient carrier capture from the wetting layer into the QDs when a high incident excitation condition was used. The first excited states in InAs/InP QDs were detected under the same condition, which demonstrates their zero-dimensional quantum states enhanced by lateral confinements. These states have a fast decay time of about 60 ps. The authors believe that their results demonstrate the possibility of fabricating performance-improved injection lasers at 1.55 μm for optical communication.

The demand for 1.3 μm low-cost laser modules for the applications in subscriber networks and optical interconnection systems has increased significantly. However, the major problem in the present laser module is the thermoelectric cooler, which is essential in most of the modules using the conventional 1.3 μm GaInAsP-InP lasers as these have poor temperature characteristics. This item not only makes the module expensive and complicated but also may degrade its long-term reliability.

Lasers emitting at 1.3 μm with better temperature characteristics are therefore in great demand. H.Wada *et al* [8] (Oki Electric Industry Company, Japan) studied the effects of well number on temperature characteristics in 1.3μm AlGaInAs-InP compressively strained multi-quantum well lasers. It was found that the temperature characteristics of the threshold current (T_0) and the maximum operation temperature (T_{max}) increased with increasing number of quantum wells. A record T_{max} of 220°C was achieved in lasers with 10 wells. However, the temperature characteristics of the external efficiency were found to decrease on increasing the number of wells. Power measurements were also carried out in order to clarify the above results.

Also, lasers working in the 1.8-2.1 μm emission range have found important applications in pumping holmium (Ho) ion crystal lasers and semiconductor lasers in the mid-infrared region. They also show potential applications in remote sensing, medical uses and eye-safe illumination. X.He *et al* [9] (Opto Power Corporation, USA) have fabricated high-power, high-efficiency lasers from a 1 cm wide GaInAsP-InP monolithic diode array lasing at 1.9 μm. Continuous-wave (CW) optical power of 13.5 W was achieved using a higher-capacity thermal-electric cooler. A life-test of 5000 hours was obtained, indicating that the arrays operate reliably at 7 W at 20°C and 6 W at 30°C.

In the last 10 years there has been a lot work in reducing the cavity volume of microcavity lasers, which offer the possibility of producing ultra-low threshold currents and large spontaneous emission factors. Microdisks were proposed as a promising candidate in order to achieve ultra-small cavities due to the simple geometry and fabrication process.

The lasing in current injection microdisk lasers has so far been demonstrated only for GaInAsP-InP [10] and GaInAs-GaAs [11] systems. However, these structures were very complex and difficult to measure. Although the threshold current is typically lower than 1 mA, lasing was obtained only under pulsed conditions. M. Fujita *et al* [12] (Yokohama National University, Japan) analysed the lasing characteristics of GaInAsP-InP current injection microdisk lasers of 2-3 μm in diameter. They achieved room temperature CW operation in a 3 μm diameter device with a record low threshold current of 150 μA (see Figures 3 and 4). This is due to the reduction of the threshold current density, which was attributed to the small scattering loss at disk sidewalls reduced by the improved ECR etching. The spontaneous emission factor was estimated to be $6x10^{-3}$.

The uni-travelling-carrier (UTC) photodiode has been proposed for high-output and high-speed photodetectors needed for 20-40 Gbits/s optical and optical-link microwave/millimetre-wave transmission systems that incorporate

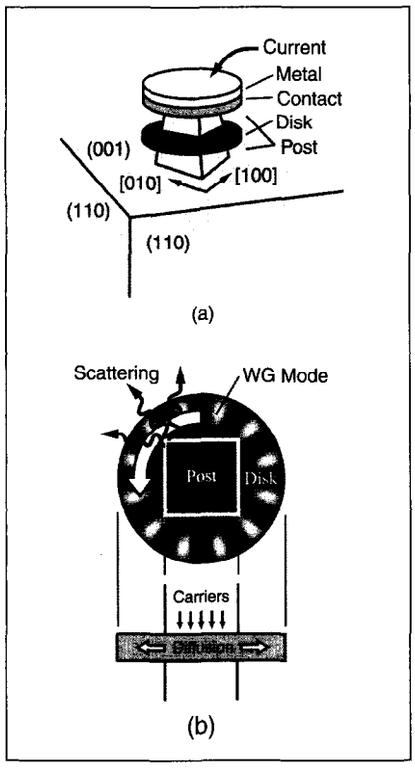

Figure 3: Schematic of microdisk injection laser: (a) overview, (b) top-view and side-view. (Courtesy of M.Fujita, Yokohama National University, Japan)

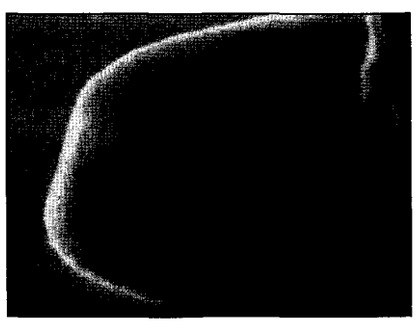

Figure 4: Magnified view of formed disk edge. (Courtesy of M.Fujita, Yokohama National University, Japan)

optical amplifiers.The UTC structure uses only electrons as active carrier. This has the benefit of reducing the space-charge effect, which is the origin of low saturation currents in conventional PIN photodetectors. M.Yuda *et al* [13] (NTT, Japan) have recently reported results obtained in a UTC waveguide photodiode which uses a semi-insulating InP buried structure (see Figures 5 and 6). It was found that the product of the photocurrent and applied voltage, which indicates the allowable level of input power, was four times higher than that of a polyimide-passivated mesa structure.Their device has a product of about 120 mW (23.5 mA x 5 V), a responsivity of 0.7 A/W, and a bandwidth of 47 GHz.

The display device technology is divided into two main areas.The first involves the III-V technology used mainly for GaAs vertical-cavity surface-emitting LEDs (VCSELs) with FET devices of high performance, expensive materials and small-area dimensions. The second area, which uses large-area substrate materials like glass or polymers with low performance Si-TFT devices, produces large-area displays for consumer applications. III-V materials, which would produce higher mobilities than Si-TFTs, were not used because:

(1) there is no evaluation of FET devices grown on low-grade highly dislocated material, and
(2) III-V layers grown below 450°C contain a high intrinsic antisite defect density.

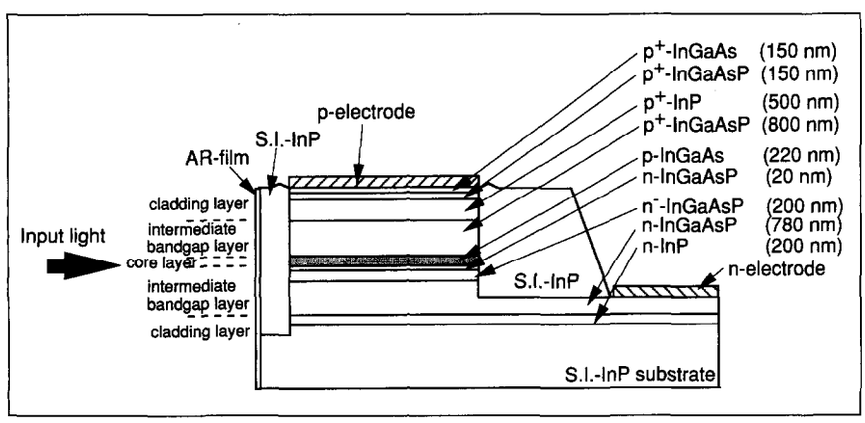

Figure 5: Cross-sectional view of a buried UTC waveguide photodiode structure in a waveguide direction. (Courtesy of M.Yuda, NTT, Japan)

A new approach to merge high-performance III-V materials properties with optical large-area display technology has been demonstrated by M. Kunze *et al* [14] at the University of Ulm, Germany.They have shown how to transfer the growth of Low Temperature Growth (LTG)-InP channel FETs to GaAs substrates (growth temperature was lower than 300°C). This result opens up the possibility of transferring this structure to Si and other substrate materials. The device structure consisted of:

(1) 60 nm LTG-AlInAs buffer layer on GaAs substrate,
(2) 55 nm LTG-InP active channel layer, and
(3) 20 nm LTG-AlInAs gate contact layer.

The RF measurements show that their devices have cut-off frequencies which are dominated by parasitic. The authors hope to improve further these characteristics by redesigning the structure. However, these preliminary results act as a starting point for growth on other non-InP substrates.

In recent years there has been a revival of experimental and theoretical interest in resonant tunnelling devices, largely motivated by the impressive progress achieved in MBE and MOVPE. Improvements in the sample quality have led to the observation of negative differential resistance at room temperatures, and have also increased the peak-to-valley ratios in the current-voltage characteristics. Tunnelling is the fastest charge transport mechanism in semiconductors. In addition, the combination of integrated circuits with resonant tunnelling diodes (RTDs) and HEMTs, for example, has led to systems which exhibit high-speed capabilities, low power consumption, and multi-functionality in logic circuits.

The GaInAs/AlAs system on InP substrates is the most promising for RTD devices because InP-based electron devices show the highest speed. Moreover, AlAs barriers on

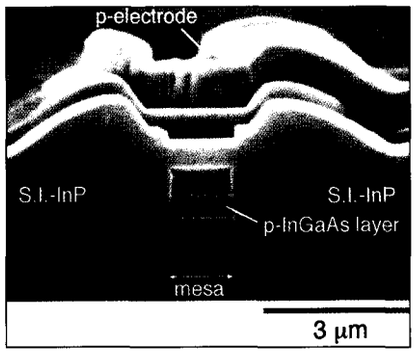

Figure 6: SEM photograph of buried mesa cross section in a direction perpendicular to waveguide. (Courtesy of M.Yuda, NTT, Japan)

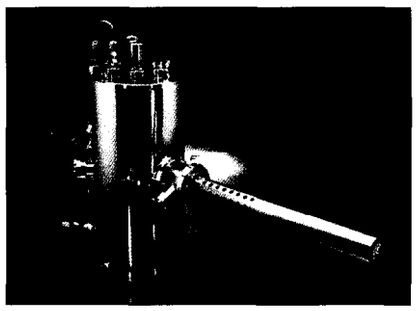

Figure 7: Valved cracker for Phosphorous. (Courtesy of EPI)

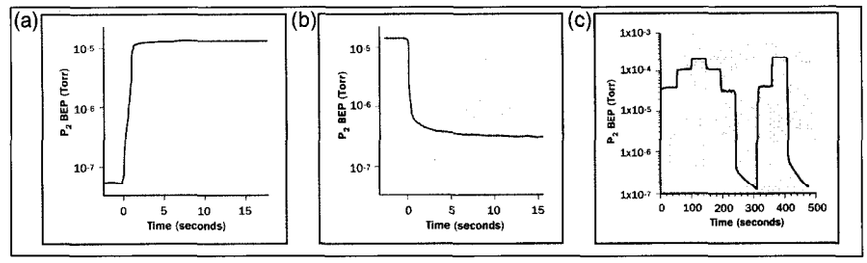

Figure 8: P_2 flux response immediately after (a) opening and (b) closing the valve (Courtesy of T.P.Chin, Purdue University, USA). (c) Modulation of P_2 beam equivalent pressure from the EPI P-valved cracker showing stability and reproducibility. (Courtesy of G.Wicks, University of Rochester, USA and EPI)

InP show a high peak-to-valley current ratio (PVR) at room temperature. Y. Miyamoto *et al* [15] (Tokyo Institute of Technology, Japan) reported on GaInAs/AlAs/InP RTDs grown by MOVPE, which has superior characteristics in productivity and uniformity as a method for fabricating InP-related devices. The dependence of barrier thickness on peak current density and uniformity was also investigated. The peak current density observed ranged from 100 to 0.1 A/cm^2. According to the authors, these results suggest that MOVPE offers the possibility of fabricating RTDs with a wider peak current density range than those devices grown by MBE. It is worth noting that RTD structures are usually grown by MBE in order to obtain abrupt heterointerfaces.

The concept of a heterostructure bipolar transistor (HBT) was first proposed in 1948. In recent years, the HBT has emerged as a leading contender to satisfy the needs in communication and information processing systems that require implementation of very high-performance electronic circuits. AlGaAs/GaAs devices have already been introduced in wireless communication systems. The InP-based HBT is another promising type of device which has demonstrated excellent high-frequency performance and has been used in various ICs for electronic and optoelectronic applications.

The recent work of D. Sawdai and D. Pavlidis [16] (University of Michigan, USA) introduced another method to improve power performance by developing a PNP HBT technology and combining the PNP HBTs with NPN HBTs in a push-pull amplifier in the InP material system. The PNP HBTs demonstrated 10 dB of gain and output power that scaled well with HBT area at 10 GHz. Both the simulations and experiments showed an improvement to the linearity characteristics of NPN HBT amplifiers by including a PNP HBT in a push-pull configuration. The authors believe that integration of NPN and PNP HBTs offers other benefits such as higher gain and less power consumption in small-signal amplifier stages through the use of active loads. In addition, such complementary amplifiers could lead to improved wireless communication systems.

Phosphorous-based devices grown by MBE

Solid-source molecular beam epitaxy (SSMBE) has recently been demonstrated as a viable alternative to MOCVD for the growth of P-based devices. While it has been well established that, for example, AlGaInP-based quantum well lasers grown by MOCVD can demonstrate low threshold currents and high output powers, previous MBE-grown device performance has typically lagged behind.

Solid phosphorus exists in two allotropic forms, referred to as red and white phosphorus. White phosphorous is highly reactive and flammable in air. Therefore, red phosphorous is the preferred form for loading in solid-source MBE.

However, due to a particularly low sublimation coefficient, red phosphorus exhibits appreciable flux transients when used in a standard valved cracker source. The solution is a multi-zone crucible to permit loading of red phosphorus, followed by an in-situ conversion to white phosphorus. The sublimation coefficient of white phosphorus is high enough to permit valved source operation with no detectable flux transients. A valved cracker designed for in-situ phosphorus conversion for the use in MBE growth has been available from EPI (see Figure 7) for a number of years. Recent enhancements have further improved the performance of this source. Excellent flux stability with negligible shutter-related transients, improved material quality, and longer system run times are now attainable (see Figure 8).

In the following I will report some results which demonstrate the successful growth of sensitive P-containing quaternary materials using a P-valved cracker cell.

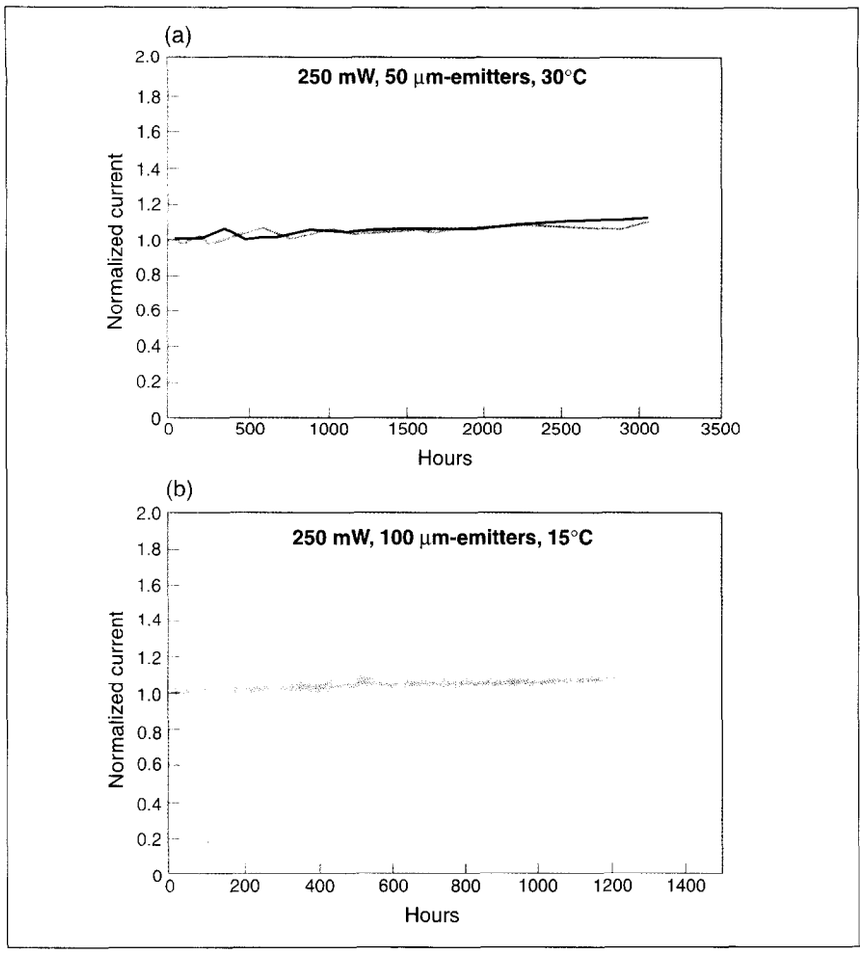

Figure 9: High-power life-tests for a group of (a) 670 nm lasers at 30°C and (b) 650 nm at 15°C. The light output power is kept constant at 250 nW in both cases. (Courtesy of of M. Toivonen et al, Tampere University, Finland and EPI)

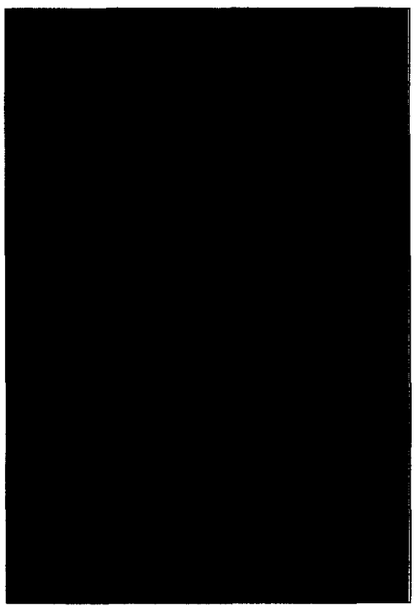

Figure 10: GaInP laser operating at 670 nm grown using an EPI valved cracker as the P_2 source. (Courtesy of G.Wicks, University of Rochester, USA and EPI)

High-power red laser diodes (600 nm range) based on strained GaInP/AlGaInP quantum well structures have been grown by SSMBE using an EPI valved cracker (see Figure 10). Output power levels of 3 W for the 670 nm, 2 W for the 650 nm, and 1 W for the 630 nm lasers have been achieved in CW mode. The lasers were processed into broad-area 50-100 μm wide oxide stripe devices, and cleaved into bars of varying cavity lengths (from 600 to 1600 μm).

Threshold current densitites as low as 350, 508, and 680 A/cm^2 for 670, 650, and 630 nm lasers, respectively, were obtained at L = 1 mm, as measured at room temperature in pulsed mode. Preliminary life-tests for the 670 nm and 650 nm lasers indicate good reliability. Eight of the 670 nm lasers with 50 μm oxide stripes were burned-in (100 hours) and then driven at a constant light power of 250 mW at 30°C. Over 3000 hours, some gradual degradation is observed but no sudden failure is indicated. Four of the 650 nm lasers with 100 μm oxide stripes (tested over 1200 hours at 250 mW at 15°C) show a degradation rate of less than 10%. Life-testing results are shown in Figure 9.

The high power outputs and good device lifetimes that were demonstrated indicate the purity of the SSMBE-grown material.

SSMBE has also been used to grow resonant cavity light-emitting diodes (RCLEDs) operating at 660 and 1300 nm. The potential applications of RCLED include high-bandwidth plastic optical fibre local-area networks, densely packed two-dimensional arrays for monochromatic displays, lighting, and high-resolution printing.

The 660 nm RCLED showed significant improvement in wall-plug efficiency and CW light output power over a standard commercial high-brightness red LED. The 1300 nm RCLED is believed to be the first reported monolithic RCLED at this wavelength.

SSMBE is demonstrated to be suitable for achieving the many abrupt steps required for these advanced structures. The 1300 nm RCLEDs were grown on 2° off towards (110) 2" n-InP substrates. The structure featured an active region with three 80Å-thick compressively-strained InAsP quantum wells and 120Å-thick GaInAsP barriers.The active region is sandwiched between GaInAsP/InP DBRs. Even without cooling, no significant deterioration in the device characteristics was observed with increasing drive current. A narrow peak width (full width half max) of 13 nm was achieved. With the red RCLEDs, peaks as narrow as 5 nm are obtained.

The high-power red laser diodes and RCLEDs reported here were grown at the Tampere University of Technology (Tampere, Finland).

Table 1.

Basic parameters at 300K	
Crystal structure	Zinc Blende
Number of atoms in 1 cm^3	$3.96x10^{22}$
Debye temperature	425 K
Density	425 $g.cm^{-3}$
Dielectric constant	12.5 (Static), 9.61 (High frequency)
Effective electron mass	0.08 m_0
Effective hole masses	0.6 m_0 (Heavy), 0.089 m_0 (Light)
Lattice constant	5.8687Å
Band structure and carrier concentration	
Energy gap	1.344 eV
Energy separation	$E_{\Gamma L}$=0.59 eV; $E_{\Gamma X}$=0.85 eV
Intrinsic carrier concentration	$1.3x10^7$ cm^{-3}
Intrinsic resistivity	$8.6x10^7$ Ω.cm
Effective conduction band density of states	$5.7x10^{17}$ cm^{-3}
Effective valence band density of states	$1.1x10^{19}$ cm^{-3}
Electrical properties	
Breakdown field	~$5x10^5$ Vcm^{-1}
Mobility	≤5400 $cm^2V^{-1}s^{-1}$ for electrons; ≤200 $cm2V^{-1}s^{-1}$ for holes
Diffusion coefficient	≤130 cm^2s^{-1} for electrons; ≤5 cm^2s^{-1} for holes
Optical properties	
Infrared refractive index	3.1
Radiative recombination coefficient	$1.2x10^{-10}$ cm^3s^{-1}
Thermal properties	
Melting point	1060°C
Thermal conductivity	0.68 Wcm^{-1} $°C^{-1}$
Thermal diffusivity	0.372 cm^2s^{-1}
Thermal expansion, linear	$4.6x10^{-6}$ $°C^{-1}$
Temperature properties	
E_g (Energy gap) (eV)=1.421 - $4.9x10^{-4}$ x $T^2/(T+327)$; 0≤T(K)≤800	
$E_{\Gamma X}$ (eV)= 0.96 - $3.7x10^{-4}$ x T; 0≤T(K)≤300	
Effective density of states in the conduction band: N_c~ $1.1x10^{14}$ x $T^{3/2}$ (cm^{-3})	
Effective density of states in the valence band: N_v~ $2.2x10^{15}$ x $T^{3/2}$ (cm^{-3})	
Dependence on hydrostatic pressure P in kbar:	
$E_g(eV)=E_g(0)$ + $8.4x10^{-3}$ x P - $1.8x10^{-5}$ x P^2	
$E_L(eV)=E_L(0)$ + $4.6x10^{-3}$ x P	
$E_X(eV)=E_X(0)$ + $2x10^{-3}$ x P	

Conclusion

The most important step in the progress of InP-based devices has been the development of high-quality materials growth. While sophisticated growth and processing facilities necessary for state-of-the-art InP device realisation are more readily available in industry, contributions to the technology from academia have been crucial in their rapid progress.

Worth noting is that InP-based HBTs have several advantages over their GaAs-based counterparts due to the differences in their material properties. GaInAs has higher electron mobility, and GaInAs and InP have higher peak electron velocities and saturated electron velocities than GaAs. So a short word of advice to those still working in the field of GaAs HBTs: it is time to switch to InP.

Also, at many sites, solid-source MBE is now preferred over gas-source MBE or MOCVD, since comparable material quality can be obtained without the cost and difficulty of handling toxic gases.

References

[1] H.Li *et al*, Appl. Phys. Lett., **75** 1173 (1999)
[2] A.G.Norman *et al*, Appl. Phys. Lett., **73** 1844 (1998)
[3] V.M.Ustinov *et al*, Appl. Phys. Lett., **72** 362 (1998)
[4] S.Frechengues *et al*, Appl. Phys. Lett., J. Crystal Growth, **201/202**
[5] D.Lacombe *et al*, Appl. Phys. Lett., **74** 1680 (1999)
[6] S.Frenchengues *et al*, Appl. Phys. Lett., **74** 3356 (1999)
[7] S.Hinooda *et al*, Appl. Phys. Lett., **75** 3530 (1999)
[8] H.Wada *et al*, IEEE J. Selected Topics in Quantum Electronics, **5** 420 (1999)
[9] X.He *et al*, Electronics Letters, **35** 1343 (1999)
[10] A.F.J.Levi *et al*, Electronics Letters, **28** 1010 (1992)
[11] C.Gmachl *et al*, IEEE J. Quantum Electron., **33** 1567 (1997)
[12] M.Fujita *et al*, IEEE J. Selected Topics in Quantum Electronics, **5** 673 (1999)
[13] M.Yuda *et al*, Electronics Letters, **35** 1377 (1999)
[14] M.Kunze *et al*, Solid State Electronics, **43** 1535 (1999)
[15] Y.Miyamoto *et al*, Solid State Electronics, **43** 1395 (1999)
[16] D.Sawdai and D.Pavlidis, Solid State Electronics, **43** 1507 (1999)

Contact: Dr M.Henini
School of Physics and Astronomy
University of Nottingham
Nottingham NG7 2RD, UK
Tel/Fax: +44 115 951 5195/5180
e-mail: mohamed.henini@nottingham.ac.uk